

Preparation and Properties of Opaque Polyethylene Terephthalate/TiO₂ Filaments

Zhaolin LIU^{1,3,4}, Yang YANG², Yuwen WANG⁴, Xuehui GAN⁵, Ni WANG^{4*}

¹ College of Textile and Garment, Hebei University of Science and Technology, Shijiazhuang 050018, China

² The Institute of Equipment Technology, Academy of People's Armed Police, Beijing 100012, China

³ Hebei Textile and Garment Technology Innovation Center, Shijiazhuang 050018, China

⁴ Key Laboratory of Science & Technology of Eco-Textile, Ministry of Education, College of Textiles, Donghua University, Shanghai 201620, China

⁵ College of Mechanical Engineering, Donghua University, Shanghai 201620, China

crossref <http://dx.doi.org/10.5755/j02.ms.24524>

Received 04 November 2019; accepted 20 January 2020

The opaque polyethylene terephthalate (PET) filaments with 0 % to 9 % mass fractions of TiO₂ particles were prepared by low-speed melt spinning and drafting. Basic structures including surface morphology, linear density, orientation degree and crystallinity, and properties including tensile and optical property of the PET/TiO₂ filaments were systematically analyzed, especially the visual shielding property. The results showed that TiO₂ particles were well-distributed on the filament surface at 3 % TiO₂ mass fraction, whereas agglomeration of TiO₂ particles appeared when the mass fraction of TiO₂ reached to 6 % and 9 %. The addition of TiO₂ increased the linear density of the PET filaments. The orientation degree of the filaments was positively correlated with the drafting ratio but hardly influenced by the mass fraction of TiO₂. The crystallinities achieved the maximum of 60.72 % and 54.99 % at the draw ratios of 3.5 and 4.0 respectively when the mass fraction of TiO₂ was 3 %, and then decreased gradually to 38.5 % or 34.74 % at 9 % TiO₂ mass fraction. The tenacities of the filaments reduced to 20.41 % and 25.50 % with the increasing TiO₂ content at the draw ratios of 3.5 and 4.0 respectively. However, the elongation at break enhanced as the TiO₂ content changed from 0 % to 3 % and then decreased to 42.53 % and 27.22 % respectively at the draw ratios of 3.5 and 4.0 with the increasing TiO₂ content. The opaque effect of the PET filaments improved significantly when the mass fraction of TiO₂ was less than 6 %, whereas the improvement of the opaque effect slowed down as the mass fraction of TiO₂ increased further.

Keywords: PET filament, TiO₂, tensile property, visual shielding property.

1. INTRODUCTION

The aims for wearing clothes have expanded with the development of society and scientific technology, while for warmth and shielding are remaining the most primary and basic purposes the same as before. Up to now, research on the fabrication and shielding property of clothes is still very limited. Only the visual shielding characteristics of silk fabrics were concerned. Li et al. [1] discussed the defilade property of silk fabrics and found that the special structure made the crepe de Chine fabric have excellent visual shielding property. Based on the relationship between color elements (lightness, hue and purity) and visual shielding property of the fine silk fabrics, Jiang et al. [2] concluded that color cooperation of the terrace clothing had influence on the visual shielding property, which was the best if colors of the inner and outer clothing were of complementary hue. The continual thinning of yarn fineness results in the lack of visual shielding more and more serious. Therefore, it is necessary to take efficient measures to improve the visual shielding property of fabrics and maintain their light weight, color and comfortability simultaneously. It is worth noting that the visual shielding property could be affected by fibers, yarn or fabric structures, and finishing due to the complexity of textiles. However, structure change is difficult to meet high

visual shielding requirement and finishing often deteriorates comfort of the fabrics. Thus, application of opaque fibers is considered to be the most feasible and effective approach to enhance visual shielding [3, 4].

It is known that the visual shielding property could be improved through the reduction of light transmittance by means of intensifying light absorption and scattering. Since the light absorption coefficient of a certain material is constant and particles with high absorption coefficient are usually not suitable for the preparation of opaque fibers, how to maximize light scattering by adding particles has become the key point to obtain opaque fibers [5]. According to Mie scattering theory, the relative refractive index of a particle is a fundamental parameter influencing the scattering power, besides the particle size, shape and surface roughness. Most of the opaque fibers are produced by adding high refractive index mineral fillers, such as TiO₂, amorphous silica and silicates, aluminum trihydrate and ZnO, among which TiO₂ is of particular attractiveness owing to its white color and high stability. Solbrig et al. [6] studied the physical and morphological change of PET yarns hydrolyzed with NaOH and containing four concentrations of TiO₂ delusterants as 0, 0.1 %, 0.3 % and 2.0 %, respectively. They found that all the PET yarns showed progressive weight loss with the increasing hydrolysis time. Yarn tenacity began to deteriorate but there was no change in crystallinity after 6 h of hydrolysis. Surface morphology of the yarns with TiO₂ differed from that without TiO₂ additive. Huang et al. [7] blended TiO₂

* Corresponding author. Tel.: +86-21-67792717; fax: +86-21-67792627. E-mail address: wangni@dhu.edu.cn (N. Wang)

into PET fibers at different proportions to make semi-finished products by melt spinning. The structures of TiO₂ on fiber surface were explored by the scanning electron microscopy and energy dispersive X-ray spectroscopy. The results indicated that TiO₂ could be evenly distributed on the fiber surface. Zhu et al. [8] pointed out that PET integrated with TiO₂ nanoparticles could have a lower crystallization temperature and melting point compared with pure PET. The TiO₂ nanoparticles after surface treatment have relatively less influence on the PET lattice matrix. Han et al. [9] prepared PET/nano TiO₂ composite fibers by adding rutile TiO₂ into the system via in situ polymerization. It was found that rutile TiO₂ dispersed in the matrix uniformly when the mass fraction of TiO₂ was 1%. Compared with pure PET fibers, PET/nano TiO₂ composite fibers exhibited lower breaking strength, lower elongation at break and crystalline. Furthermore, the fabrics had splendid screening effect against UVA and UVB with an ultraviolet protection factor above 50.

For the development of opaque PET filaments, the mass fraction of TiO₂ is much higher than that in the semi-dull or dull PET filaments [10]. However, there is little research related to the effect of high percentage TiO₂ on the structures and properties of opaque PET filaments, especially the visual shielding property. In this study, opaque PET filaments added with different mass fractions of TiO₂ particles were prepared by low-speed melt spinning and drafting. The basic structures including surface morphology, linear density, orientation and crystallinity, and the properties including tensile and visual shielding of the opaque PET filaments were systematically investigated. Close attention was paid to the visual shielding property.

2. EXPERIMENTAL DETAILS

2.1. Materials

The materials used included fiber-grade PET chips with an intrinsic viscosity of 0.69 dL/g and high TiO₂ containing PET master batch, both of which were provided by Zhejiang Xinxin Chemical Fiber Co., Ltd. (China). TiO₂ particles were well dispersed in the PET matrix with a mass fraction of 50% in the PET master batch.

2.2. Preparation of PET/TiO₂ filaments

PET chips and master batch were first pre-crystallized by DGG-9070 electric thermostat blast drying oven. The temperature began at 90 °C and increased by every 10 °C per hour until 120 °C for the maintenance of 2 h. The pre-crystallized chips were then dried at 155 °C for 48 h to make the moisture content lower than 50 ppm by JM-500ZGX dynamic vacuum dryer. The PET chips and master batch were blended in proportion to match the ratio listed in Table 1. Mass fractions of the added TiO₂ were 0, 3, 6, 9%, respectively.

Table 2. Melt spinning parameters of the PET/TiO₂ filaments

Samples	Screw extruder temperatures, °C				Spin pump temperature, °C	Bending tube temperature, °C	Spin head temperature, °C
	I	II	III	IV			
TiO ₂ -0, TiO ₂ -3, TiO ₂ -6, TiO ₂ -9	282	300	295	295	295	295	293

The undrawn yarns (UDY) were spun on ABE-25 spinning frame with a speed of 800 m/min. The obtained UDY were drawn on a TF-100 parallel-draft machine with the draw ratio of 3.5 and 4.0, respectively. Temperatures of the hot plate and hot disc were set as 80 °C and 160 °C. Detailed parameters of the melting spinning process are given in Table 2. The resultant PET/TiO₂ filaments prepared with various TiO₂ mass fractions and different drawing ratios were denoted as TiO₂-x/DR-y.

Table 1. Mass fractions of PET and TiO₂ in the PET/TiO₂ filaments

Mass fraction of PET chips, %	Mass fraction of master batch, %	Mass fraction of TiO ₂ , %
100	0	0
94	6	3
88	12	6
82	18	9

2.3. Characterization

Morphologies of the PET/TiO₂ filaments were observed by JSM-5600LV scanning electron microscopy (SEM). The filaments were sputter-coated with a gold layer of 10 nm thickness before scanning and the acceleration voltage was 15 kV.

After humidity-adjustment under the standard condition of 65% relative humidity and 20 °C, the linear density of the PET filaments was calculated according to the relationship between weight and length. Orientation degree of the PET filaments was measured on SCY-III fiber sound velocimeter developed by Shanghai Donghua Ltd., China. X-ray diffraction (XRD) patterns were evaluated on the D/max-2550P X-ray diffractometer to calculate the crystallinity. The CuKα radiation with a wave length of 1.542 nm was generated at 40 kV and 200 mA. All the samples were scanned at the speed of 20 °/min in the 2θ ranging from 3 ° to 60 °.

Tensile properties of the filaments were tested using YG061 tensile test machine with a gauge length of 500 mm and a speed of 500 mm/min. The tenacity, initial modulus and elongation at break were obtained by calculating the average value of 30 trials for each sample.

The visual shielding effect of the opaque PET filaments was evaluated by Hitachi U-4100 Ultraviolet Visible Near-Infrared Spectrophotometer. The filaments were wrapped around a transparent glass slide in turn. Each filament was strictly controlled to wind 90 laps within the length of 3.5 cm and maintain uniform tension during the winding process. The scanning was ranged from 350 nm to 800 nm with a speed of 300 nm/min and a resolution of 2 nm. The transmission and reflection spectra of the PET filaments with various TiO₂ mass fractions were obtained.

3. RESULTS AND DISCUSSION

3.1. Surface morphology

Fig. 1 shows the SEM images of the PET filament surfaces with 0 %, 3 %, 6 % and 9 % TiO₂ at the draw ratio of 3.5, where the gray areas and white dots represent the PET matrix and TiO₂ particles respectively. It can be seen that surface of the pure PET filament is smooth. TiO₂ particles are well dispersed on the filament surface without forming significant aggregation when the mass fraction of TiO₂ is 3 %. As the mass fraction of TiO₂ reaches to 6 % and 9 %, agglomeration of TiO₂ particles can be observed.

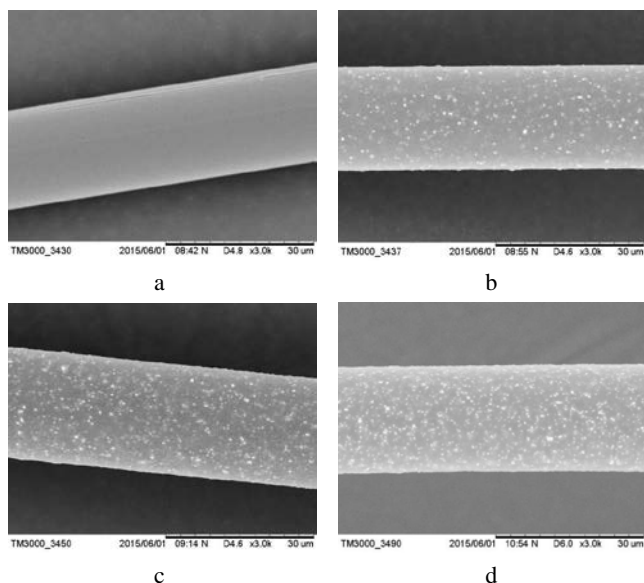


Fig. 1. SEM images of the PET filament surfaces at the draw ratio of 3.5 with different mass fractions of TiO₂: a–0 % TiO₂; b–3 % TiO₂; c–6 % TiO₂; d–9 % TiO₂

3.2. Linear density

Linear densities of the PET filaments are demonstrated in Fig. 2. Because the density of anatase TiO₂ is 3.8–3.9 g/cm³, much larger than that of PET [11], therefore, the linear densities of the filaments with the addition of TiO₂ show an increasing tendency compared with pure PET filaments. On the other hand, the higher is the draw ratio, the smaller is the linear density.

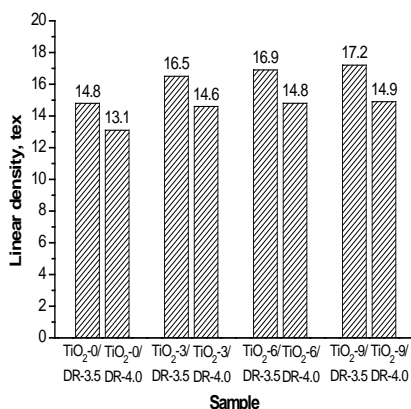


Fig. 2. Linear densities of the PET filaments with different mass fractions of TiO₂ and draw ratios

3.3. Orientation degree and crystallinity

The orientation factor of the PET filaments with different mass fractions of TiO₂ and draw ratios is listed in Table 3. It could be concluded that draw ratio has significant influence on the orientation degree of PET filament. The macromolecular chains are arranged in parallel along the direction of external force with the increasing draw ratio, thus the orientation factor of the macromolecular chains of the filaments becomes larger with the increase of draw ratio. However, there seems no obvious law between the orientation degree of the filaments and the mass fraction of TiO₂.

The XRD patterns of the PET filaments are given in Fig. 3. It can be seen clearly that new curves appear after the addition of TiO₂ at 2θ equals to 38°, 48°, 54° and 55°. Both the increase of TiO₂ mass fraction and the draw ratio have nothing to do with the position of the curves. Compared with the results of the standard PDF card of TiO₂, it can be concluded that the new curves come from the anatase type of TiO₂.

The calculated crystallinity of the PET filaments is listed in Table 3. No matter the draw ratios are 3.5 or 4.0, the crystallinity of the PET filaments enhances as the TiO₂ mass fraction changes from 0 % to 3 %, and then decreases as the TiO₂ mass fraction continues to augment. When a small amount of TiO₂ is added into the PET filaments, the TiO₂ particles act as the nucleating agent and PET molecules are inclined to form regular alignment of the crystalline region. As a result, the crystallinity shows a rising trend initially. However, when the TiO₂ content exceeds 6 %, the large amount of TiO₂ plays the role of cross-linking, making the PET molecular chains difficult to slip along external force and leading to the reduction of crystallinity.

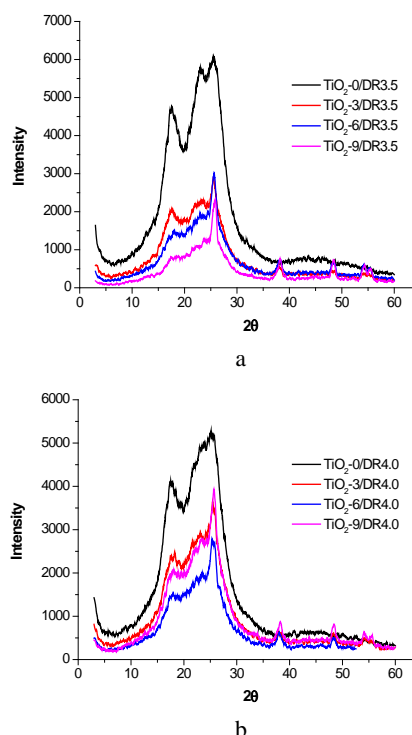


Fig. 3. XRD patterns of the PET filaments with different mass fractions of TiO₂ and draw ratios

Table 3. Orientation factor and crystallinity of the PET filaments with different mass fractions of TiO₂ and draw ratios

Sample	TiO ₂ -0/ DR-3.5	TiO ₂ -0/ DR-4.0	TiO ₂ -3/ DR-3.5	TiO ₂ -3/ DR-4.0	TiO ₂ -6/ DR-3.5	TiO ₂ -6/ DR-4.0	TiO ₂ -9/ DR-3.5	TiO ₂ -9/ DR-4.0
Orientation factor	0.7993	0.8911	0.8134	0.8864	0.8194	0.8864	0.8220	0.8653
Crystallinity, %	30.28	34.75	60.72	54.99	47.89	38.07	38.5	34.74

3.4. Tensile property

The tensile property of the PET filaments are displayed in Table 4. The tenacity shows a gradual declination with the increase of TiO₂ mass fraction, while the elongation at break has a nonlinear relationship with the TiO₂ content.

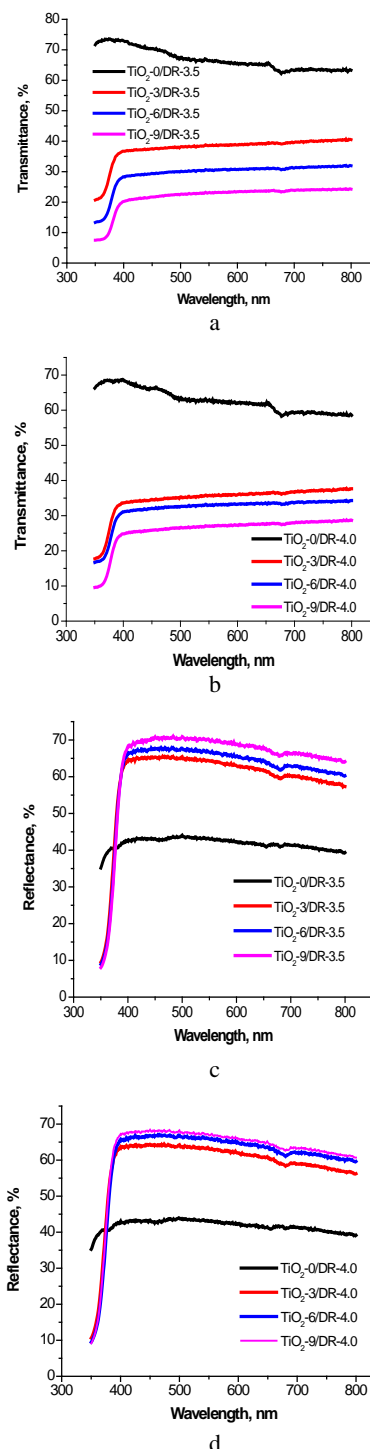
On one hand, the TiO₂ particles could reduce the interaction force between the PET macromolecular chains. On the other hand, the intensified TiO₂ aggregation at high TiO₂ mass fraction results in the deterioration of interfacial defects and the aggravation of stress concentration. That is why the tenacity of the PET filaments decreases with the growing TiO₂ content. Similar conclusions have been obtained from the study of PA6/POE-g-MAH/nano SiO₂ composites and PA66/Mica composites [12, 13].

The elongation at break of the PET filaments improves when the mass fraction of TiO₂ is 3 % and then reduces with the TiO₂ mass fraction, but the variation is rather slight overall. The initial increase of the elongation at break can be ascribed to the ball-like role playing by the small amount of TiO₂, which weakens the interaction force between PET molecular chains and makes the relative slip between molecular chains easy to produce. On the contrary, brittleness of the PET filaments would increase as the content of TiO₂ reaches 6 %, leading to the drop of the elongation at break. From the analysis above, in order to maintain necessary strength and toughness of the opaque PET filaments, the mass fraction of TiO₂ should be carefully regulated.

3.5. Visual shielding property

The transmission and reflection spectra of the PET filaments with different mass fractions of TiO₂ and draw ratios are shown in Fig. 4. It can be found that the light transmittance of the PET filaments diminishes while the light reflectance increases with the increasing mass fraction of TiO₂ at both the draw ratios of 3.5 and 4.0. Furthermore, the changes of light transmittance and light reflectance tend to be more obvious when the TiO₂ mass fraction ranges from 0 % to 3 % than those when the TiO₂ mass fraction is within 3 % to 9 %.

The transmittance of pure PET filaments is up to 73.6 % at the draw ratio of 3.5 but drops to below 40.6% when the TiO₂ mass fraction is 3 %. Similarly, the transmittance of pure PET filaments is as high as 68.7 % at the draw ratio of 4.0 and decreases to less than 37.7 % when the TiO₂ mass fraction is 3 %, meaning the overall opaque effect of the filaments is significantly enhanced after adding a tiny amount of TiO₂. The interface between PET molecular chains and TiO₂ enlarges as more TiO₂ particles are added, resulting in more light reflection and scattering.

**Fig. 4.** Transmission and reflection spectra of the PET filaments with different mass fractions of TiO₂ and draw ratios

The path through which light is transmitted extends correspondingly, therefore, the transmittance of the PET filaments decreases with the increasing TiO₂ mass fraction.

The reflectance of the PET filaments increases significantly after the addition of TiO₂, since the refractive index of TiO₂ is much higher than that of PET. Similar result has been acquired when we studied the influence of TiO₂ on the optical property of PET films [14]. Both the decrease of light transmittance and the increase of light reflectance can improve the opaqueness of the PET filaments effectively.

Table 4. Tensile properties of the PET filaments with different mass fractions of TiO₂ and draw ratios

Sample	Tenacity, cN/tex	Elongation at break, %	CV of tenacity, %
TiO ₂ -0/DR-3.5	24.36	41.51	4.72
TiO ₂ -0/DR-4.0	30.78	28.63	1.97
TiO ₂ -3/DR-3.5	22.53	45.03	5.07
TiO ₂ -3/DR-4.0	26.60	29.47	3.78
TiO ₂ -6/DR-3.5	21.83	44.52	5.65
TiO ₂ -6/DR-4.0	25.59	28.24	4.21
TiO ₂ -9/DR-3.5	20.41	42.53	3.74
TiO ₂ -9/DR-4.0	25.50	27.22	3.21

4. CONCLUSIONS

The opaque PET filaments were prepared by melt spinning and drafting with the addition of TiO₂ particles. The structures and properties of the opaque PET filaments were systematically analyzed and the following conclusions can be drawn:

1. TiO₂ particles dispersed evenly on the surface of PET filaments when the mass fraction of TiO₂ was less than 3 %, and then TiO₂ agglomerated as the mass fraction of TiO₂ reached to 6 % and 9 %.
2. The orientation degree of the PET filaments was positively correlated with the draw ratio. However, the change of orientation degree was not obvious with the addition of TiO₂. The crystallinity achieved the peak value when TiO₂ mass fraction was 3 %, and then decreased as the TiO₂ mass fraction continued to grow.
3. The tenacity of the PET filaments showed a gradual declination with the increase of TiO₂ mass fraction. Whereas the elongation at break raised when the mass fraction of TiO₂ was 3 %, and then reduced with the addition of TiO₂.
4. The transmittance of the PET filaments decreased sharply and the reflectance of the PET filaments intensified as the content of TiO₂ was 3 %. Therefore, the opaque effect of the PET filaments improved significantly. When the content of TiO₂ ranged from 6 % to 9 %, the variation of the transmittance and reflectance tended to be slight, making the improvement of the opaque effect slow down.

Acknowledgments

This work is supported by the National Key R&D Program of China (2016YFB0302703), National Natural Science Foundation of China (51804096), 2020 Undergraduates Innovation Program of Hebei Province (S202010082019).

REFERENCES

1. **Jiang, H., Li, D., Chen, Y.** Investigation on a Derlade Property of Silk Fabric *Journal of Suzhou Institute of Silk Textile Technology* 14 (4) 1994: pp. 26–31.
2. **Jiang, H., Zhong, H.** A Colour Cooperate Method for Improving Defilade Property of Fine Silk Fabric *Journal of Suzhou Institute of Silk Textile Technology* 14 (4) 1994: pp. 33–43.
3. **Wang, N., Pan, W., Shi, M., Yu, J.** Theoretical Analysis on the Development of Opaque Fibers based on Mie Scattering *Textile Research Journal* 83(4) 2013: pp. 355–362. <https://doi.org/10.1177/0040517512452947>
4. **Shi, M., Qiu, Y., Zhang, Y., Wang, N.** Study on the Visual Masking Property of the Textiles *Textile Science Research* 6 (3) 2008: pp. 19–23.
5. **Wang, N., Liu, Z., Shi, M., Yu, J.** Effect of Wearing Characteristics on Visual Shielding Property of Woven Fabrics *Fibers and Polymers* 16 (3) 2015: pp. 685–690. <https://doi.org/10.1007/s12221-015-0685-6>
6. **Solbrig, C.M., Obendorf, S.K.** Alkaline Hydrolysis of Titanium Dioxide Delustered Poly (ethylene terephthalate) Yarns *Textile Research Journal* 61 (3) 1991: pp. 177–181. <https://doi.org/10.1177/004051759106100308>
7. **Huang, Y., Tang, J., Chang, F.** Effect of PET Melt-spinning on TiO₂ Nanoparticle Aggregation and Friction Behavior of Fiber Surface *Industrial & Engineering Chemistry Research* 48 (17) 2007: pp. 5548–5544. <https://doi.org/10.1021/ie070248y>
8. **Zhu, X., Wang, B., Chen, S.** Synthesis and Non-isothermal Crystallization Behavior of PET/Surface-treated TiO₂ Nanocomposites *Journal of Macromolecular Science Part B-Physics* 47(6) 2008: pp. 1117–1129. <https://doi.org/10.1080/00222340802403206>
9. **Han, K., Yu, M.** Preparation and Properties of PET/Nano Titanium Dioxide Ultraviolet Resistant Fiber *Synthetic Fiber Industry* 28(2) 2005: pp. 4–9. <https://doi.org/10.3969/j.issn.1001-0041.2005.02.002>
10. **Wang, N., Cao, X., Hu, J., Shi, M.** Development of Opaque Fibers and Its Application in Wool Fabrics *Wool Textile Journal* 41(3) 2013: pp. 1–6. <https://doi.org/10.3969/j.issn.1003-1456.2013.01.001>
11. **Gao, L., Zheng, S., Zhang, Q.** Nano Titanium Dioxide Photo Catalytic Materials and Applications. Chemical Industry Press, Beijing, 2002: pp. 89–91.
12. **Chen, H., Wang, G., Huang, Y., Zeng, X., Chen, J.** Morphology and Mechanical Properties of PA6/POE-g-MAH/Nano SiO₂ Composites *Plastics* 36(6) 2007: pp. 21–24. <https://doi.org/10.3969/j.issn.1001-9456.2007.06.006>
13. **Gao, Y., Cui, W., Ren, L., Lei, N.** Study on Properties of PA-6/Mica Composite and PA-6/Treated-mica Composite *New Chemical Materials* 41(3) 2013: pp. 26–28. <https://doi.org/10.3969/j.issn.1006-3536.2013.03.009>
14. **Wang, N., Liu, Z., Shi, M., Yu, J.** Effect of the Filled Titanium Dioxide Particulates on Optical Properties of Polyester Films *The Journal of the Textile Institute* 108(5) 2017: pp. 776–782. <https://doi.org/10.1080/00405000.2016.1190497>



© Liu et al. 2021 Open Access This article is distributed under the terms of the Creative Commons Attribution 4.0 International License (<http://creativecommons.org/licenses/by/4.0/>), which permits unrestricted use, distribution, and reproduction in any medium, provided you give appropriate credit to the original author(s) and the source, provide a link to the Creative Commons license, and indicate if changes were made.